LABORATOIRE DE PHYSIQUE MOLECULAIRE ET APPLICATIONS

Université Pierre et Marie Curie
Tour 13 - Bte 76 - 4, Place Jussieu
75252 PARIS Cedex 05 (France)
Fax : (1) 44.27.38.54 - Tél. : (1) 44.27.....



# SCIENTIFIC REPORT

## Line Intensities and Self-Broadening Coefficients of $^{12}C^{16}O_2$ and $^{13}C^{16}O_2$ Lines in the Laser Band Region

Grant AFOSR-90-0364



V. DANA

Laboratoire de Physique Moléculaire et Applications,
Centre National de la Recherche Scientifique,
Université Pierre et Marie Curie, Tour 13, Bte 76,
4, Place Jussieu, 75252 PARIS CEDEX 05, France

CURITY CLASSIFICATION OF THIS PAGE

# REPORT DOCUMENTATION PAGE

Form Approved
OMB No. 0704-0188

| | |
|---|---|
| 1a. REPORT SECURITY CLASSIFICATION<br>Unclassified | 1b. RESTRICTIVE MARKINGS |
| 2a. SECURITY CLASSIFICATION AUTHORITY | 3. DISTRIBUTION/AVAILABILITY OF REPORT<br>Approved for public release ; Distribution unlimited |
| 2b. DECLASSIFICATION/DOWNGRADING SCHEDULE | |
| 4. PERFORMING ORGANIZATION REPORT NUMBER(S) | 5. MONITORING ORGANIZATION REPORT NUMBER(S)<br>EOARD TR 92-06 |
| 6a. NAME OF PERFORMING ORGANIZATION<br>CNRS - Lab. de Physique Moléculaire & Applications<br>6b. OFFICE SYMBOL (If applicable)<br>LDG | 7a. NAME OF MONITORING ORGANIZATION<br>EOARD |
| 6c. ADDRESS (City, State, and ZIP Code)<br>Bte 76 - Tour 13 - Université P. & M. Curie<br>4 Place Jussieu<br>75252 PARIS CEDEX 05, France | 7b. ADDRESS (City, State, and ZIP Code)<br>223/231 Old Marylebone Rd<br>London NW1 5TH UK |
| 8a. NAME OF FUNDING/SPONSORING ORGANIZATION<br>European Office of Aerospace Research and Development<br>8b. OFFICE SYMBOL (If applicable)<br>LDG | 9. PROCUREMENT INSTRUMENT IDENTIFICATION NUMBER<br>AFOSR-90-0964 |
| 8c. ADDRESS (City, State, and ZIP Code)<br>223/231 Old Marylebone Rd<br>London NW1 5TH UK | 10. SOURCE OF FUNDING NUMBERS<br>PROGRAM ELEMENT NO. 61102 F; PROJECT NO. 2301; TASK NO D1; WORK UNIT ACCESSION NO. |

11. TITLE (Include Security Classification)
Line intensities and self-broadening coefficients of $^{12}C^{16}O_2$ and $^{13}C^{16}O_2$ lines in the laser band region

12. PERSONAL AUTHOR(S)
V. DANA

| 13a. TYPE OF REPORT | 13b. TIME COVERED | 14. DATE OF REPORT (Year, Month, Day) | 15. PAGE COUNT |
|---|---|---|---|
| FINAL | FROM Sept 90 TO SEPT91 | 1992,03,25 | 28 |

16. SUPPLEMENTARY NOTATION

| 17. COSATI CODES | | | 18. SUBJECT TERMS (Continue on reverse if necessary and identify by block number) |
|---|---|---|---|
| FIELD | GROUP | SUB-GROUP | Intensities, Self-broadening, laser band |
| | | | |

19. ABSTRACT (Continue on reverse if necessary and identify by block number)

The intensities of $^{12}C^{16}O_2$ and $^{13}C^{16}O_2$ lines have been measured in the laser band regior (around 10 μm), using Fourier transform spectra. For each studied band the square of the transition dipole moment and Herman-Wallis coefficients have been determined.

The band intensities deduced from these results are in good agreement with those obtaine by the Direct Numerical Diagonalization calculations. In addition the self broadening coefficients have been measured.

| 20. DISTRIBUTION/AVAILABILITY OF ABSTRACT | 21. ABSTRACT SECURITY CLASSIFICATION |
|---|---|
| ☒ UNCLASSIFIED/UNLIMITED ☐ SAME AS RPT. ☐ DTIC USERS | Unclassified |
| 22a. NAME OF RESPONSIBLE INDIVIDUAL<br>Janet C. JOHNSTON | 22b. TELEPHONE (Include Area Code)<br>44-71-409-4437 / 22c. OFFICE SYMBOL<br>LDG |

DD Form 1473, JUN 86 Previous editions are obsolete SECURITY CLASSIFICATION OF THIS PAGE

# SCIENTIFIC REPORT

## Line Intensities and Self-Broadening Coefficients of $^{12}C^{16}O_2$ and $^{13}C^{16}O_2$ Lines in the Laser Band Region

Grant AFOSR-90-0364

V. DANA

Laboratoire de Physique Moléculaire et Applications,
Centre National de la Recherche Scientifique,
Université Pierre et Marie Curie, Tour 13, Bte 76,
4, Place Jussieu, 75252 PARIS CEDEX 05, France

This report is divided into two parts: the first part is devoted to the methodology of the measurements and to the $^{12}C^{16}O_2$ molecule, and the second part to the $^{13}C^{16}O_2$ isotopic species.

## PART I

## Line intensities and self-broadening coefficients of $^{12}C^{16}O_2$ lines in the laser band region. Methodology of the measurements

**SUMMARY**

The intensities of $^{12}C^{16}O_2$ lines have been measured in the four bands centered at 927.156, 960.959, 1063.735, and 1071.542 $cm^{-1}$, using Fourier transform spectra. The square of the transition dipole moment and Herman-Wallis coefficients have been determined; the band intensities deduced from these results are in good agreement with those obtained by the Direct Numerical Diagonalization calculations. In addition, the self-broadening coefficients of 90 lines have been measured in the two strongest bands.

## I. INTRODUCTION

In its laser band region, the main isotopic species of carbon dioxide gives rise mainly to four parallel hot bands around 10$\mu$m. Among them, the strongest are the 00011-10001 and 00011-10002 bands centered respectively at 960.959 and 1063.735 $cm^{-1}$, the other two being the 01111-11101 and 01111-11102 weak bands centered respectively at 927.156 and 1071.542 $cm^{-1}$. The last published experimental results concerning these bands are those of Abubakar and Shaw (see Ref. (1) and its bibliography where the references of ealier works can be found). The last intensity calculations are those of Wattson and Rothman (2), who used a Direct Numerical Diagonalization method (hereafter denoted as DND). At the present time, the data available through the 1986 version of the HITRAN database (3) are currently used for various radiative transfer studies.

We present here the results of systematic measurements of line intensities in the four above-mentioned bands. High resolution Fourier transform spectra (unapodized FWHM = $2.7 \times 10^{-3}$ $cm^{-1}$) have been used to retrieve accurate absolute line and band intensities, and it appeared that our results compare better with the last DND calculated values (2) than with the 1986 HITRAN values (3). The self-broadening coefficients of 90 lines pertaining to the two strongest bands were also measured: they do not reveal any vibrational dependence.

## II. EXPERIMENTAL DETAILS

The intensities and self-broadening coefficients measurements were performed on five spectra recorded with the Fourier transform spectrometer of the Laboratoire de Physique Moléculaire et Applications, at the Université Paris-Sud. The experimental conditions are summarized in Table I.

The length of the absorption path inside the White-type cell is very well known. The pressure has been measured with an uncertainty of 0.1 Torr. So, the uncertainties on these two quantities (≈ 0.1% on the absorption path and ≈ 0.2% on the gas pressure) have very small effects on the retrieved line parameters. On the contrary, since we are studying hot bands, it is necessary to know the temperature with a good accuracy. The temperature was measured in three places: in the room, on the cell walls, and inside the cell. The equality of the three measured values has shown that a thermal equilibrium had been reached during the recording of each interferogram. However, as a recording takes around ten hours, small variations of the temperature occur. The values of the temperatures reported in Table I are average values which define the temperature of our measurements with a maximum uncertainty of ± 1 K.

## III. METHOD OF MEASUREMENTS

### III.1. Treatment of the channeled spectra

In the studied spectral region, fringes, caused by multiple optical reflections on the opposite sides of the beam splitter, appear on the spectra. Figures 1 and 2 show portions of typical channeled spectra. The presence of a channel of this type is a source of difficulties in the treatment of the spectra, since it has been proved that it could hardly affect the line positions and intensities (4, 5). In recent works (see, *e.g.*, Refs. (6, 7)), a channel observed on spectra has been taken into account in the treatment. However, we have to point out the fact that the fringes we are dealing with in this work come from multiple reflections inside the interferometer; they have not to be confused with fringes due to multiple reflections on the filter or on the windows of the apparatus. In the following, we will discuss how we have removed the channel from our spectra, without introducing additional errors.

In Ref. (5), it has been shown that the second reflection on the sides of the beam splitter gives rise to two secondary interferograms in addition to the main interferogram $I(\Delta)$, and that the actual recorded interferogram is

$$I'(\Delta) = I(\Delta) + \gamma_1 I(\Delta-\delta) + \gamma_2 I(\Delta+\delta), \qquad (1)$$

where $\Delta$ is the path difference between the fixed and moving mirrors, and $\delta$ the path difference between the opposite sides of the beam splitter ($\gamma_1$ and $\gamma_2$ are related to the reflection and transmission coefficients of the sides of the beam splitter). From Eq. (1), one can deduce (5) the expression of the transmission $T(\sigma)$, resulting from an isolated absorption line of profile $g(\sigma-\sigma_0)$ centered at $\sigma_0$:

$$\begin{aligned} T(\sigma) = T_b(\sigma) \{ & [1-g(\sigma-\sigma_0)] * f(\sigma\Delta_{max}) \\ & + 2\,\gamma_2 \cos(2\pi\sigma\delta) * f(\sigma\Delta_{max}) \\ & - [g(\sigma-\sigma_0)\ (\gamma_1+\gamma_2) \cos(2\pi\sigma\delta)] * f(\sigma\Delta_{max}) \end{aligned}$$

$$- [g(\sigma-\sigma_0)\ (\gamma_1-\gamma_2)\ \sin(2\pi\sigma\delta)] * h(\sigma\Delta_{max})\}, \quad (2)$$

where the symbol * represents a convolution product. $T_b(\sigma)$ is the low resolution enveloppe: since its variation is very weak along a line, it has not be included in the convolution product, so in the following, in order to simplify the notation, $T(\sigma)$ will represent the ratio $T(\sigma)/T_b(\sigma)$. $f(\sigma\Delta_{max})$ and $h(\sigma\Delta_{max})$ are the symmetrical and antisymmetrical apparatus functions respectively (8):

$$f(\sigma\Delta_{max}) = 2\ \Delta_{max}\ \sin(2\pi\sigma\Delta_{max})\ /\ 2\pi\sigma\Delta_{max}, \quad (3)$$

and $$h(\sigma\Delta_{max}) = 2\ \Delta_{max}\ [1-\cos(2\pi\sigma\Delta_{max})]\ /\ 2\pi\sigma\Delta_{max}, \quad (4)$$

$\Delta_{max}$ being the maximum path difference.

Equation (2) is the complete expression of a channeled spectrum. The first term between braces is the usual unchanneled spectrum. The second term represents the sine channel observable on the continuous background (note that because of small variations of the beam splitter indices with the wavenumber, the amplitude and the period of the experimental channel can change very slightly along the spectrum). The second and third terms of Eq. (2) perturb the line depth and can cause errors in line intensity measurements if they are not taken into account in the analysis. The fourth term leads to an asymmetry in the line shape; it can cause noticeable errors in line position measurements (8).

In absence of absorbing gas, only the second term and the constant in the first term of Eq. (2) are different from zero. Since in usual experimental conditions the period of the channel is much larger than the resolution limit, one can write the expression of the channel in absence of absorption as $T_0(\sigma)$

$$T_0(\sigma) = 1 + 2\ \gamma_2\ \cos(2\pi\sigma\delta). \quad (5)$$

In the vicinity of each studied line, $T_0(\sigma)$ can be obtained fitting the continuous background by Eq. (5) on wide domains on each side of the studied line, where the influence of this line and of the neighboring ones is negligible ($\leq 0.1\%$). Moreover, Eq. (5)

shows that ratioing the channeled spectrum (Eq. 2) against an empty cell background exhibiting the same channel (Eq. 5) puts the channel out of sight on the resulting plotted spectrum, but is not sufficient to avoid errors in line positions and intensities, since only the second term of Eq. 2 has been removed.

A similar problem occurs in the zero transmission determination from saturated lines. Indeed, on the top of such a line, considering that $g(\sigma-\sigma_0)$ remains constant (equal to 1) on a spectral domain much larger than the resolution limit, one can write the expression of the trasmission as $T_s(\sigma)$:

$$T_s(\sigma_0) = (\gamma_2-\gamma_1)\ \cos(2\pi\sigma_0\delta). \qquad (6)$$

This expression shows that the transmission $T_s(\sigma_0)$ around the center of a saturated line depends on the position of this line with respect to the channel, as can be seen on Fig. 2. Consequently, spectra with saturated lines can be advantageously used to obtain the variation $T_s(\sigma)$ of the true zero transmission level with the wavenumber. Practically, wide sets of broad saturated lines, having various positions with respect to the channel, were used to obtain $T_s(\sigma)$ from the experimental data through a least squares fit. Thus, we could check that:

- first, $T_s(\sigma)$ is actually well described by a sine function;
- and second, $T_0(\sigma)$ and $T_s(\sigma)$ have the same phase, according to the usual values (5) of $\gamma_1$ and $\gamma_2$; also, the ratio of their amplitudes is constant along each spectrum.

All this suggests the following procedure to treat correctly a channeled spectrum. Equations (2,5,6) lead to:

$$t(\sigma) = [T(\sigma) - T_s(\sigma)] \ / \ [T_0(\sigma) - T_s(\sigma)] \qquad (7)$$

$$\# \ [1-g(\sigma-\sigma_0)] \ * \ [f(\sigma\Delta_{max}) + \rho\ h(\sigma\Delta_{max})], \qquad (8)$$

$$\text{with} \quad \rho = [(\gamma_1-\gamma_2)\ \sin(2\pi\sigma_0\delta)] \ / [1+(\gamma_1+\gamma_2)\ \cos(2\pi\sigma_0\delta)]. \qquad (9)$$

Since the values observed for $|\rho|$ are very small (typically, less than 0.1), Eq. (1) can formally be rewritten as:

$$t(\sigma) = [1-g(\sigma-\sigma_0)] * q(\sigma-\sigma_0) \qquad (10)$$

with

$$q(\sigma\Delta_{max}) = [\cos\phi\ f(\sigma\Delta_{max}) + \sin\phi\ h(\sigma\Delta_{max})], \qquad (11)$$

$\sin\phi = \rho$, and $\cos\phi \# 1$.

$t(\sigma)$ represents the convolution of the absorption line by an asymmetrical apparatus function $q(\sigma\Delta_{max})$; the spectrum is correctly dischanneled, contrary to that happens when one performs the ratio $T(\sigma)/T_0(\sigma)$. For each line the effective apparatus function $q(\sigma\Delta_{max})$ depends on a parameter $\phi$; this parameter plays a similar role than the parameter describing a phase error (8).

Practically, $T_0(\sigma)$ and $T_s(\sigma)$ are measured on the spectra as explained above, and the values of $t(\sigma)$ are obtained using Eq.(7) at each primary point of the spectrum.

### III.2. The apparatus function

As said above, a correct treatment of $t(\sigma)$ needs the use of an asymmetrical apparatus function. The parameter $\phi$ in $q(\sigma\Delta_{max})$ is adjusted for each line according to its position with respect to the channel, in order to reach the best fit. It was checked in Ref. (8) that it is necessary to take into account the effect of the parameter $\phi$, to avoid relative errors of few percents in the intensity and line width measurements.

Furthermore, to obtain accurate line intensities and widths, it is advisable to take into account the slight apodization due to the trough-put. In a previous work (9), we had established an analytical expression for the symmetrical apodized apparatus function. This expression was used in Eq. (11) in place of $f(\sigma\Delta_{max})$.

### III.3. The fitting procedure

To obtain the line parameters, a spectrum, computed using Eq.(10), is adjusted, for each primary point, to the experimental

values of $t(\sigma)$ (determined as explained in Section III.1). In Eq. (10), the apparatus function described in Section III.2 was used. $g(\sigma-\sigma_0)$ is the absorption line shape under infinite resolution:

$$g(\sigma-\sigma_0) = \exp[-S°PL\ (1/\gamma^D)\ (Log2/\pi)^{1/2}\ k(x,y)], \qquad (12)$$

with $S°$ = line intensity,
$P$ = pressure of the absorbing gas,
$L$ = length of the absorbing path,
$\gamma^D$ = Doppler half-width,
$\gamma^L$ = Lorentz half-width,
$x = (Log2)^{1/2}\ (\sigma-\sigma_0)\ /\ \gamma^D$,
$y = (Log2)^{1/2}\ \gamma^L\ /\ \gamma^D$,

and where $k(x,y)$ is the reduced Voigt profile calculated with the aid of the Gautschi's algorithm (10).

The intensity of some lines are missing since it was impossible to fit the channel in their vicinity, because of the presence of neighboring lines.

## IV. DATA REDUCTION AND DISCUSSION OF THE RESULTS

### IV.1. Line intensities

Using the method detailed in the previous section, we have measured more than 160 line intensities in the laser bands region of $^{12}C^{16}O_2$. The five spectra (Table I) have been used, and we checked that the lines which could be measured simultaneously in different spectra gave results in good agreement (discrepancy smaller than 2 %). Moreover, no systematic discrepancy appeared between the sets of line intensities deduced from different spectra.

Our results are reported in Tables II-V according to the bands; the intensites have been converted to cm/mol-unit at the reference temperature of the HITRAN database, *i.e.*, 296 K. The uncertainty on these intensities will be discussed now. The treat-

ment of the channel avoid large errors on the line parameters determination, but it decreases slightly the signal to noise ratio. The residuals of the fits are mainly due to the noise. On the average, the statistical relative uncertainties on the obtained intensities is 2 %. An additional uncertainty comes from the uncertainty on the temperature (see Section II): several tests showed us that an error of 0.5 K on the temperature does not change the intensities by more than 2 %. On the whole, a maximum value of the uncertainty on our absolute line intensities is about 5 %.

For each band, we have derived the square of the transition dipole moment $|\mu|^2$, with respect to the running index m (m = -J" in the P branch and J"+1 in the R branch, J" being the rotational quantum number of the lower level). $|\mu|^2$ can be expressed as $|\mu|^2 = |\mu_0|^2 F(m)$, where $|\mu_0|^2$ is the vibrational dipole moment matrix element and F(m) the F-factor including Herman-Wallis coefficients:

$$F(m) = [1 + A_1 m + A_2 J"(J"+1)]^2. \qquad (13)$$

In addition, the relationship between the intensity of a transition between states i and f, $S_{if}$, and $|\mu|^2$ is given by:

$$S_{if}(T) = (8\pi^3/3hc)\ \sigma_{if}\ [1 - \exp(-c_2\sigma_{if} / T)]\ (I_a/Q(T)) \times \exp(-c_2 E_i / T)\ L_{if}\ |\mu|^2\ 10^{-36}, \qquad (14)$$

where $\sigma_{if}$ is the frequency of the transition, $c_2$ is the second radiation constant (hc/k), $I_a$ is the natural isotopic abundance, Q(T) is the total internal partition sum, and $E_i$ is the energy of the lower state. The units are cgs, except for $|\mu|$ which is in Debyes. The point to be noted is that in this definition the line intensities are functions of the temperature, T, and the isotopic abundance $I_a$, while $|\mu|^2$ is independent of these quantities. The transition moment constants obtained through a fit of the line intensities are reported in Table VI. Using Eq. (13), the line intensities have been calculated and compared with their experimental values (see Tables II-V). The agreement is good, as can also

be seen on Figs. 3-6.

From the usual relationship between the band intensity and the square of the transition dipole moment (2,11), we have calculated the intensities of the four studied bands. The obtained values are reported in Table VII together with the last published DND (2) and HITRAN (3) results. One can see that the DND calculated values agree better with our experimental results than with the 1986 HITRAN values. The slight discrepancies between our results and DND are smaller than our stated uncertainty (5%).

### IV.2. Self-broadening coefficients

The fitting of the line profiles can give simultaneously the line intensities and the self-broadening coefficients. This was done for the two strongest bands, but this could not be possible for the two other bands because of the weakness of the lines. For these weak hot lines, the self-broadening coefficients were constrained to approximate values, close to those measured in other bands.

The measured self-broadening coefficients are listed in Table VIII and plotted on Fig. 7. The temperature is 294 ± 1 K, and the uncertainty on absolute values is 5%. Figure 7 shows that for the two concerned bands, no vibrational dependence appears.

## V. CONCLUSION

Using Fourier transform spectra, systematic measurements of absolute line intensities have been performed in the $^{12}C^{16}O_2$ bands centered at 927.156, 960.959, 1063.735, and 1071.542 $cm^{-1}$, improving upon the previous experimental results. Also, self-broadening coefficients of lines belonging to the bands centered at 960.959 and 1063.735 $cm^{-1}$ were measured. These results concerning the laser bands region of $^{12}C^{16}O_2$ will be useful for radiative transfer studies.

**CAPTIONS OF THE TABLES**

**TABLE I.** Experimental Conditions for the $^{12}C^{16}O_2$ spectra

**TABLE II.** Line Intensities for the 00011-10001 Band of $^{12}C^{16}O_2$

**TABLE III.** Line Intensities for the 00011-10002 Band of $^{12}C^{16}O_2$

**TABLE IV.** Line Intensities for the 01111-11101 Band of $^{12}C^{16}O_2$

**TABLE V.** Line Intensities for the 01111-11102 Band of $^{12}C^{16}O_2$

**TABLE VI.** Transition Moment Constants $|\mu_0|^2$, $A_1$, and $A_2$ for $^{12}C^{16}O_2$

**TABLE VII.** Band Intensities $S_v$ of the Studied Laser Bands of $^{12}C^{16}O_2$

**TABLE VIII.** Self-Broadening Coefficients Measured for Lines of the 00011-10001 and 00011-10002 Bands of $^{12}C^{16}O_2$, in $10^{-3}$ $cm^{-1}.atm^{-1}$

TABLE I

**Radius of the iris:** 2.85 mm

**Focal length of the collimator:** 2000 mm

**Signal to Noise Ratio:** ≈ 150

**Absorbing gas:** 99.998 % minimum purity carbon dioxide in natural abundance (*i.e.* 98.4 % of $^{12}C^{16}O_2$) purchased from Air Liquide

| Spectrum number | Absorbing path (cm) | Total pressure (Torr) | Maximal path difference (cm) | Temperature (K) |
|---|---|---|---|---|
| 1 | 5217 | 49.9 | 182.37 | 294.2 |
| 2 | 5217 | 49.9 | 184.01 | 293.8 |
| 3 | 2817 | 49.9 | 175.07 | 293.8 |
| 4 | 417 | 50.0 | 184.01 | 294.7 |
| 5 | 5217 | 100.0 | 184.01 | 294.2 |

TABLE II

| Line | σ | $S_{obs}$ | $S_{cal}$ | % |
|---|---|---|---|---|
| P54 | 910.016 | 4.45 | 4.31 | 3.2 |
| P52 | 912.231 | 6.32 | 6.25 | 1.2 |
| P50 | 914.419 | 9.12 | 8.91 | 2.3 |
| P44 | 920.829 | 22.91 | 23.31 | -1.8 |
| P40 | 924.974 | 40.89 | 40.58 | 0.7 |
| P38 | 927.008 | 51.78 | 52.14 | -0.7 |
| P36 | 929.018 | 64.27 | 65.79 | -2.4 |
| P34 | 931.002 | 81.56 | 81.51 | 0.1 |
| P32 | 932.961 | 96.03 | 99.09 | -3.2 |
| P30 | 934.894 | 115.00 | 118.19 | -2.8 |
| P28 | 936.804 | 132.40 | 138.20 | -4.4 |
| P24 | 940.548 | 175.80 | 177.42 | -0.9 |
| P22 | 942.383 | 196.40 | 194.53 | 1.0 |
| P18 | 945.980 | 223.40 | 217.59 | 2.6 |
| P16 | 947.742 | 228.20 | 220.88 | 3.2 |
| P14 | 949.479 | 217.90 | 217.42 | 0.2 |
| P12 | 951.192 | 205.40 | 206.37 | -0.5 |
| P10 | 952.881 | 190.50 | 187.64 | 1.5 |
| P 8 | 954.545 | 156.80 | 161.27 | -2.9 |
| P 6 | 956.185 | 127.40 | 127.91 | -0.4 |
| P 4 | 957.801 | 87.51 | 88.85 | -1.5 |
| P 2 | 959.392 | 46.66 | 45.64 | 2.2 |
| R 0 | 961.733 | 22.47 | 22.99 | -2.3 |
| R 2 | 963.263 | 67.10 | 68.08 | -1.5 |
| R 4 | 964.769 | 110.80 | 110.39 | 0.4 |
| R 6 | 966.250 | 148.90 | 147.81 | 0.7 |
| R 8 | 967.707 | 179.30 | 179.19 | 0.1 |
| R10 | 969.140 | 204.20 | 203.26 | 0.5 |
| R12 | 970.547 | 221.70 | 219.61 | 0.9 |
| R14 | 971.930 | 229.80 | 228.10 | 0.7 |
| R16 | 973.289 | 228.40 | 229.10 | -0.3 |
| R18 | 974.622 | 224.70 | 223.37 | 0.6 |
| R20 | 975.930 | 213.70 | 212.32 | 0.6 |
| R22 | 977.214 | 198.10 | 196.81 | 0.6 |
| R24 | 978.472 | 180.40 | 178.29 | 1.2 |
| R26 | 979.705 | 159.40 | 158.05 | 0.8 |
| R28 | 980.913 | 139.00 | 137.15 | 1.3 |
| R30 | 982.096 | 119.40 | 116.70 | 2.3 |
| R32 | 983.252 | 95.90 | 97.35 | -1.5 |
| R34 | 984.383 | 77.45 | 79.71 | -2.9 |
| R36 | 985.488 | 65.55 | 64.05 | 2.3 |
| R38 | 986.567 | 51.02 | 50.54 | 0.9 |
| R40 | 987.620 | 38.85 | 39.17 | -0.8 |
| R42 | 988.647 | 29.64 | 29.81 | -0.6 |
| R44 | 989.646 | 22.46 | 22.31 | 0.7 |
| R46 | 990.620 | 17.13 | 16.39 | 4.3 |
| R48 | 991.566 | 11.60 | 11.84 | -2.0 |

| | | | | |
|---|---|---|---|---|
| R50 | 992.485 | 8.28 | 8.41 | -1.6 |
| R52 | 993.376 | 5.80 | 5.88 | -1.3 |
| R54 | 994.240 | 3.98 | 4.04 | -1.4 |
| R56 | 995.077 | 2.76 | 2.73 | 1.1 |
| R58 | 995.885 | 1.76 | 1.81 | -3.0 |

Units are $10^{-25}$ cm/mol at 296 K in natural abundance. $\sigma$ are the line positions in $cm^{-1}$. $S_{obs}$ are the measured intensities and $S_{calc}$ the intensities calculated using the transition moment constants listed in Table VI. % is the relative difference between these two values.

TABLE III

| Line | σ | $S_{obs}$ | $S_{cal}$ | % |
|---|---|---|---|---|
| P60 | 1005.477 | 2.13 | 2.08 | 2.2 |
| P56 | 1010.043 | 4.64 | 4.68 | -0.8 |
| P54 | 1023.189 | 6.86 | 6.92 | -0.9 |
| P52 | 1014.518 | 9.33 | 9.86 | -5.7 |
| P50 | 1016.721 | 13.97 | 14.05 | -0.6 |
| P48 | 1018.901 | 19.21 | 19.61 | -2.1 |
| P46 | 1021.057 | 25.56 | 26.64 | -4.2 |
| P44 | 1023.189 | 35.61 | 35.89 | -0.8 |
| P42 | 1025.298 | 47.71 | 47.53 | 0.4 |
| P40 | 1027.382 | 65.61 | 61.88 | 5.7 |
| P38 | 1029.442 | 76.48 | 79.12 | -3.5 |
| P36 | 1031.478 | 101.60 | 99.40 | 2.2 |
| P34 | 1033.488 | 123.50 | 122.95 | 0.4 |
| P32 | 1035.474 | 153.90 | 149.00 | 3.4 |
| P30 | 1037.434 | 172.80 | 176.80 | -2.3 |
| P28 | 1039.369 | 214.80 | 206.15 | 4.0 |
| P26 | 1041.279 | 242.80 | 235.55 | 3.0 |
| P24 | 1043.163 | 269.30 | 263.76 | 2.1 |
| P22 | 1045.022 | 294.90 | 288.82 | 2.1 |
| P20 | 1046.854 | 303.40 | 308.90 | -1.8 |
| P18 | 1048.661 | 315.50 | 322.21 | -2.1 |
| P16 | 1050.441 | 319.40 | 326.99 | -2.4 |
| P14 | 1052.196 | 330.10 | 322.09 | 2.4 |
| P12 | 1053.923 | 302.40 | 305.73 | -1.1 |
| P10 | 1055.625 | 287.20 | 278.35 | 3.1 |
| P 8 | 1057.300 | 246.30 | 239.45 | 2.8 |
| P 6 | 1058.949 | 189.10 | 190.28 | -0.6 |
| P 4 | 1060.571 | 131.40 | 132.26 | -0.7 |
| P 2 | 1062.166 | 66.51 | 69.04 | -3.8 |
| R 0 | 1064.509 | 33.96 | 34.49 | -1.6 |
| R 2 | 1066.037 | 104.90 | 102.48 | 2.3 |
| R 4 | 1067.539 | 162.10 | 166.57 | -2.8 |
| R 6 | 1069.014 | 221.80 | 223.95 | -1.0 |
| R 8 | 1070.402 | 271.10 | 272.78 | -0.6 |
| R10 | 1071.884 | 311.20 | 311.32 | -0.0 |
| R12 | 1073.278 | 345.50 | 337.47 | 2.3 |
| R16 | 1075.988 | 344.40 | 357.22 | -3.7 |
| R18 | 1077.302 | 354.70 | 349.62 | 1.4 |
| R20 | 1078.591 | 319.50 | 334.45 | -4.7 |
| R22 | 1079.852 | 314.70 | 312.32 | 0.8 |
| R26 | 1082.296 | 247.10 | 254.55 | -3.0 |
| R28 | 1083.479 | 223.20 | 222.93 | 0.1 |
| R30 | 1084.635 | 192.00 | 191.25 | 0.4 |
| R32 | 1085.766 | 160.70 | 161.01 | -0.2 |
| R36 | 1087.948 | 106.30 | 107.90 | -1.5 |
| R38 | 1089.001 | 86.34 | 86.05 | 0.3 |
| R42 | 1091.030 | 52.25 | 49.08 | 6.1 |
| R44 | 1092.007 | 42.57 | 39.24 | 7.8 |

| | | | | |
|---|---|---|---|---|
| R46 | 1092.958 | 29.49 | 29.20 | 1.0 |
| R48 | 1093.885 | 20.02 | 21.36 | -6.7 |
| R50 | 1094.786 | 15.21 | 15.37 | -1.1 |
| R56 | 1097.345 | 5.22 | 5.36 | -2.7 |
| R58 | 1098.149 | 3.64 | 3.49 | 4.0 |

Units are $10^{-25}$ cm/mol at 296 K in natural abundance. $\sigma$ are the line positions in $cm^{-1}$. $S_{obs}$ are the measured intensities and $S_{calc}$ the intensities calculated using the transition moment constants listed in Table VI. % is the relative difference between these two values.

TABLE IV

| Line | σ | $S_{obs}$ | $S_{cal}$ | % |
|---|---|---|---|---|
| P27 | 904.102 | 4.94 | 5.02 | -1.6 |
| P26 | 904.765 | 5.34 | 5.35 | -0.1 |
| P25 | 905.950 | 5.89 | 5.64 | 4.2 |
| P24 | 906.639 | 5.93 | 5.98 | -0.9 |
| P22 | 908.487 | 6.77 | 6.55 | 3.3 |
| P21 | 909.578 | 6.71 | 6.82 | -1.6 |
| P20 | 910.310 | 6.78 | 7.00 | -3.3 |
| P19 | 911.360 | 7.05 | 7.17 | -1.8 |
| P18 | 912.108 | 7.37 | 7.31 | 0.8 |
| P17 | 913.118 | 7.21 | 7.40 | -2.6 |
| P16 | 913.880 | 7.23 | 7.41 | -2.5 |
| P15 | 914.854 | 7.30 | 7.40 | -1.3 |
| P12 | 917.350 | 7.29 | 6.88 | 5.6 |
| P11 | 918.258 | 6.47 | 6.62 | -2.3 |
| P 9 | 919.927 | 5.92 | 5.88 | 0.8 |
| P 7 | 921.573 | 4.83 | 4.82 | 0.3 |
| P 6 | 922.366 | 4.26 | 4.19 | 1.8 |
| R 3 | 930.223 | 2.87 | 2.86 | 0.5 |
| R 8 | 933.917 | 6.15 | 6.02 | 2.1 |
| R10 | 933.350 | 6.93 | 6.87 | 0.9 |
| R11 | 936.086 | 6.97 | 7.20 | -3.3 |
| R16 | 939.496 | 8.01 | 7.80 | 2.6 |
| R19 | 941.584 | 7.80 | 7.49 | 4.0 |
| R22 | 943.412 | 6.95 | 6.77 | 2.6 |
| R27 | 946.715 | 5.13 | 5.13 | 0.0 |
| R28 | 947.096 | 4.68 | 4.78 | -2.0 |

Units are $10^{-25}$ cm/mol at 296 K in natural abundance. σ are the line positions in $cm^{-1}$. $S_{obs}$ are the measured intensities and $S_{calc}$ the intensities calculated using the transition moment constants listed in Table VI. % is the relative difference between these two values.

TABLE V

| Line | σ | $S_{obs}$ | $S_{cal}$ | % |
|---|---|---|---|---|
| P41 | 1034.412 | 2.17 | 2.16 | 0.4 |
| P39 | 1036.460 | 2.77 | 2.80 | -1.1 |
| P38 | 1036.927 | 3.19 | 3.16 | 0.8 |
| P37 | 1038.484 | 3.44 | 3.56 | -3.4 |
| P33 | 1042.462 | 5.50 | 5.47 | 0.6 |
| P31 | 1044.415 | 6.81 | 6.58 | 3.3 |
| P29 | 1046.344 | 7.75 | 7.77 | -0.3 |
| P27 | 1048.248 | 8.91 | 8.99 | -0.9 |
| P22 | 1052.702 | 11.90 | 11.85 | 0.4 |
| P20 | 1054.552 | 12.70 | 12.69 | 0.0 |
| P16 | 1058.172 | 13.30 | 13.44 | -1.0 |
| P14 | 1059.940 | 13.30 | 13.17 | 1.0 |
| P12 | 1061.681 | 12.70 | 12.50 | 1.6 |
| P11 | 1062.600 | 11.90 | 12.01 | -0.9 |
| P10 | 1063.394 | 11.20 | 11.33 | -1.2 |
| P 8 | 1065.079 | 9.78 | 9.75 | 0.3 |
| P 4 | 1068.366 | 5.15 | 5.14 | 0.1 |
| R 2 | 1073.850 | 2.64 | 2.61 | 1.3 |
| R 6 | 1076.829 | 9.16 | 9.07 | 1.0 |
| R11 | 1080.427 | 13.10 | 13.33 | -1.8 |
| R13 | 1081.820 | 13.60 | 14.02 | -3.1 |
| R18 | 1085.095 | 13.80 | 14.20 | -2.9 |
| R20 | 1086.375 | 14.20 | 13.61 | 4.2 |
| R23 | 1088.403 | 12.30 | 12.15 | 1.2 |
| R25 | 1089.645 | 11.20 | 10.88 | 2.9 |
| R27 | 1090.861 | 9.50 | 9.62 | -1.2 |
| R28 | 1091.215 | 8.75 | 8.95 | -2.2 |
| R30 | 1092.356 | 7.73 | 7.71 | 0.3 |
| R32 | 1093.470 | 6.48 | 6.41 | 1.0 |
| R38 | 1096.646 | 3.35 | 3.39 | -1.2 |

Units are $10^{-25}$ cm/mol at 296 K in natural abundance. σ are the line positions in $cm^{-1}$. $S_{obs}$ are the measured intensities and $S_{calc}$ the intensities calculated using the transition moment constants listed in Table VI. % is the relative difference between these two values.

TABLE VI

| $\sigma_0$ | Transition | $\mu_0^2$ $10^{-3}$ Debye$^2$ | $A_1$ x$10^4$ | $A_2$ x$10^5$ |
|---|---|---|---|---|
| 927.156 | 01111–11101 | 1.4344 (37) | -5.6 (20) | |
| 960.959 | 00011–10001 | 1.4395 (55) | -7.83 (41) | -1.06 (13) |
| 1063.735 | 00011–10002 | 1.1774 (24) | | 1.33 (17) |
| 1071.542 | 01111–11102 | 1.123 (66) | -1.0 (7) | |

$\sigma_o$ is the band center in cm$^{-1}$. The uncertainties are two standard deviations in units of the last digit.

TABLE VII

| $\sigma_0$ | Transition | $S_v$ This work | $S_v$ DND | %[a] | $S_v$ HITRAN'86 | %[b] |
|---|---|---|---|---|---|---|
| 927.156 | 01111–11101 | 4.14 | 4.20 | 1.4 | 4.20 | 1.4 |
| 960.959 | 00011–10001 | 61.3 | 61.5 | 0.3 | 68.7 | 12.1 |
| 1063.735 | 00011–10002 | 91.5 | 91.3 | -0.2 | 97.5 | 6.6 |
| 1071.542 | 01111–11102 | 7.57 | 7.68 | 1.5 | 7.68 | 1.5 |

Units are $10^{-23}$ cm/mol at 296 K in natural abundance. $\sigma_o$ is the band center in $cm^{-1}$. DND Comes from Ref. (2), and HITRAN'86 from Ref. (3)

[a] 100 [$S_v$(DND) - $S_v$(this work)] / $S_v$(this work)

[b] 100 [$S_v$(HITRAN'86) - $S_v$(this work)] / $S_v$(this work)

TABLE VIII

| Line | 00011–10001 | 00011–10002 |
|---|---|---|
| P54 | 71.4 | |
| P52 | 69.6 | |
| P50 | 72.8 | |
| P44 | 73.3 | 74.8 |
| P42 | | 73.9 |
| P40 | 78.6 | 77.7 |
| P38 | 78.5 | 80.4 |
| P36 | 85.0 | 83.6 |
| P34 | 84.8 | 82.7 |
| P32 | 85.5 | 88.1 |
| P30 | 88.5 | 88.1 |
| P28 | 85.4 | 90.9 |
| P26 | | 94.2 |
| P24 | 93.6 | 98.6 |
| P22 | 95.7 | 99.7 |
| P20 | | 99.2 |
| P18 | 99.5 | 99.8 |
| P16 | 102.3 | 101.1 |
| P14 | 103.0 | 103.5 |
| P12 | 107.9 | 103.7 |
| P10 | 106.8 | 108.4 |
| P 8 | 107.2 | 112.6 |
| P 6 | 111.4 | 113.3 |
| P 4 | 118.4 | 116.1 |
| P 2 | 119.7 | |
| R 0 | 129.6 | |
| R 2 | 118.2 | 118.4 |
| R 4 | 114.0 | 112.9 |
| R 6 | 110.2 | 110.3 |
| R 8 | 107.5 | 110.3 |
| R10 | 106.3 | 106.9 |
| R12 | 102.6 | 103.3 |
| R14 | 102.0 | |
| R16 | 100.6 | 103.3 |
| R18 | 98.1 | 96.4 |
| R20 | 97.4 | 97.7 |
| R22 | 95.4 | 94.4 |
| R24 | 93.8 | |
| R26 | 90.2 | 89.9 |
| R28 | 88.3 | 89.0 |
| R30 | 88.5 | 88.9 |
| R32 | 85.7 | 86.1 |
| R34 | 82.0 | |
| R36 | 79.9 | 82.2 |
| R38 | 79.8 | 80.3 |

| | | |
|---|---|---|
| R40 | 78.4 | |
| R42 | 77.9 | 77.5 |
| R44 | 73.2 | |
| R46 | 72.9 | 75.8 |
| R48 | 70.4 | 68.9 |
| R50 | 70.0 | |
| R52 | 70.5 | |
| R54 | 68.5 | |
| R56 | 66.9 | |

**CAPTIONS OF THE FIGURES**

**FIG. 1.** Portion of a channeled spectrum (number 4 of Table I), showing fringes caused by multiple optical reflections on the beamsplitter.

**FIG. 2.** The same spectral region as in Fig. 1, but with saturated lines (spectrum number 1 of Table I). Note that the zero transmission level is also affected by the channel: its true position can be obtained from the top of saturated lines.

**FIG. 3.** Variation of $|\mu|^2$ (in $10^{-2}$ Debye$^2$) vs m in the P- and R-branches of the 00011 ← 10001 band of $^{12}C^{16}O_2$. The curve represents the variation of $|\mu|^2$ calculated using the transition moment constants listed in Table VI.

**FIG. 4.** Variation of $|\mu|^2$ (in $10^{-2}$ Debye$^2$) vs m in the P- and R-branches of the 00011 ← 10002 band of $^{12}C^{16}O_2$. The curve represents the variation of $|\mu|^2$ calculated using the transition moment constants listed in Table VI.

**FIG. 5.** Variation of $|\mu|^2$ (in $10^{-2}$ Debye$^2$) vs m in the P- and R-branches of the 00111 ← 11101 band of $^{12}C^{16}O_2$. The curve represents the variation of $|\mu|^2$ calculated using the transition moment constants listed in Table VI.

**FIG. 6.** Variation of $|\mu|^2$ (in $10^{-2}$ Debye$^2$) vs m in the P- and R-branches of the 00111 ← 11102 band of $^{12}C^{16}O_2$. The curve represents the variation of $|\mu|^2$ calculated using the transition moment constants listed in Table VI.

**FIG. 7.** Variation of the self-broadening coefficients $\gamma$ of $^{12}C^{16}O_2$, in $10^{-3}$ cm$^{-1}$.atm$^{-1}$, vs |m|. The measured values have been plotted as stars for the 00011 ← 10001 band, and as open triangles for the 00011 ← 10002 band.

FIGURE 1

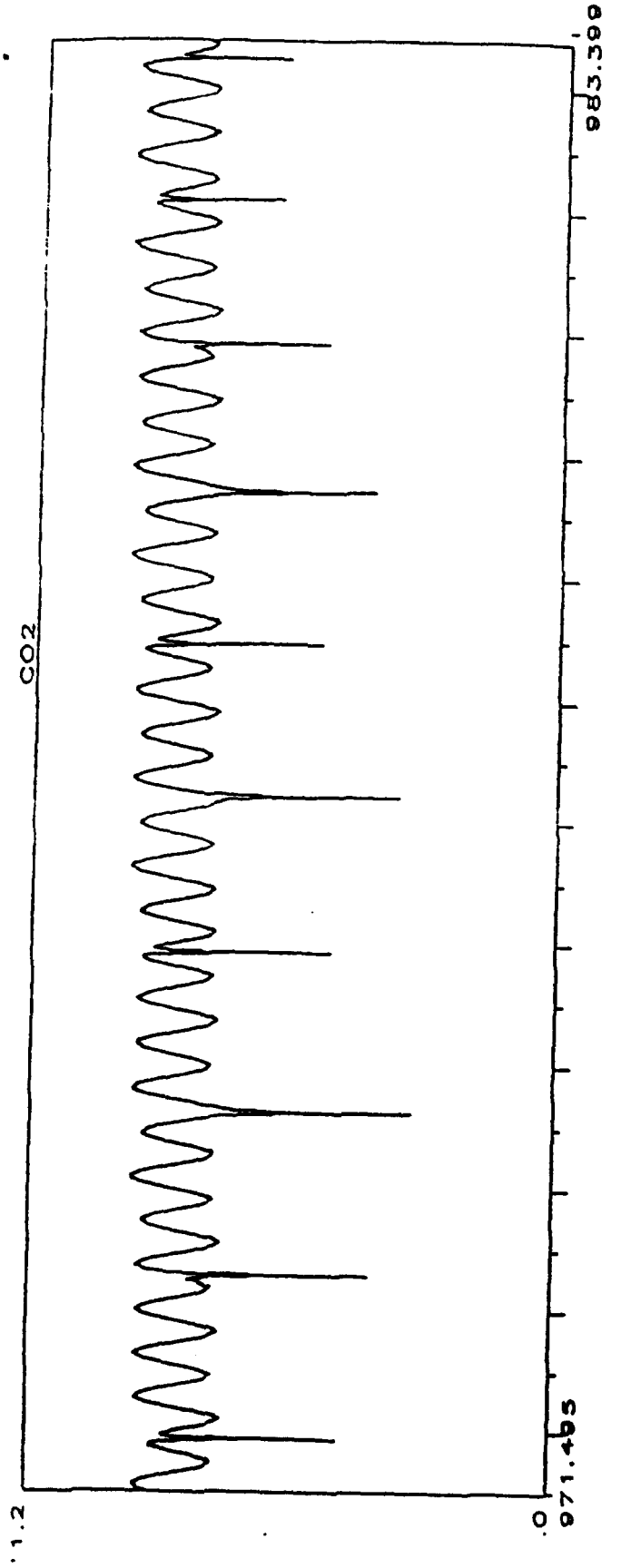


FIGURE 2

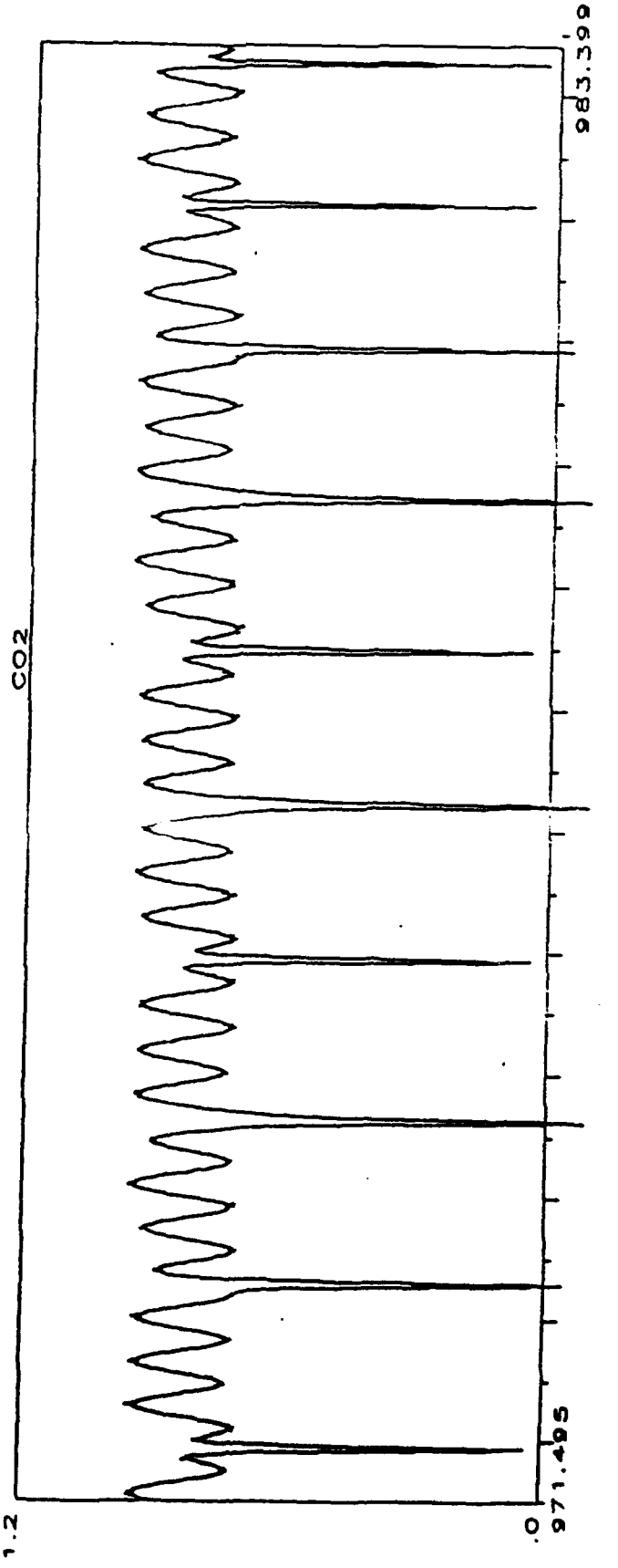

FIGURE 3

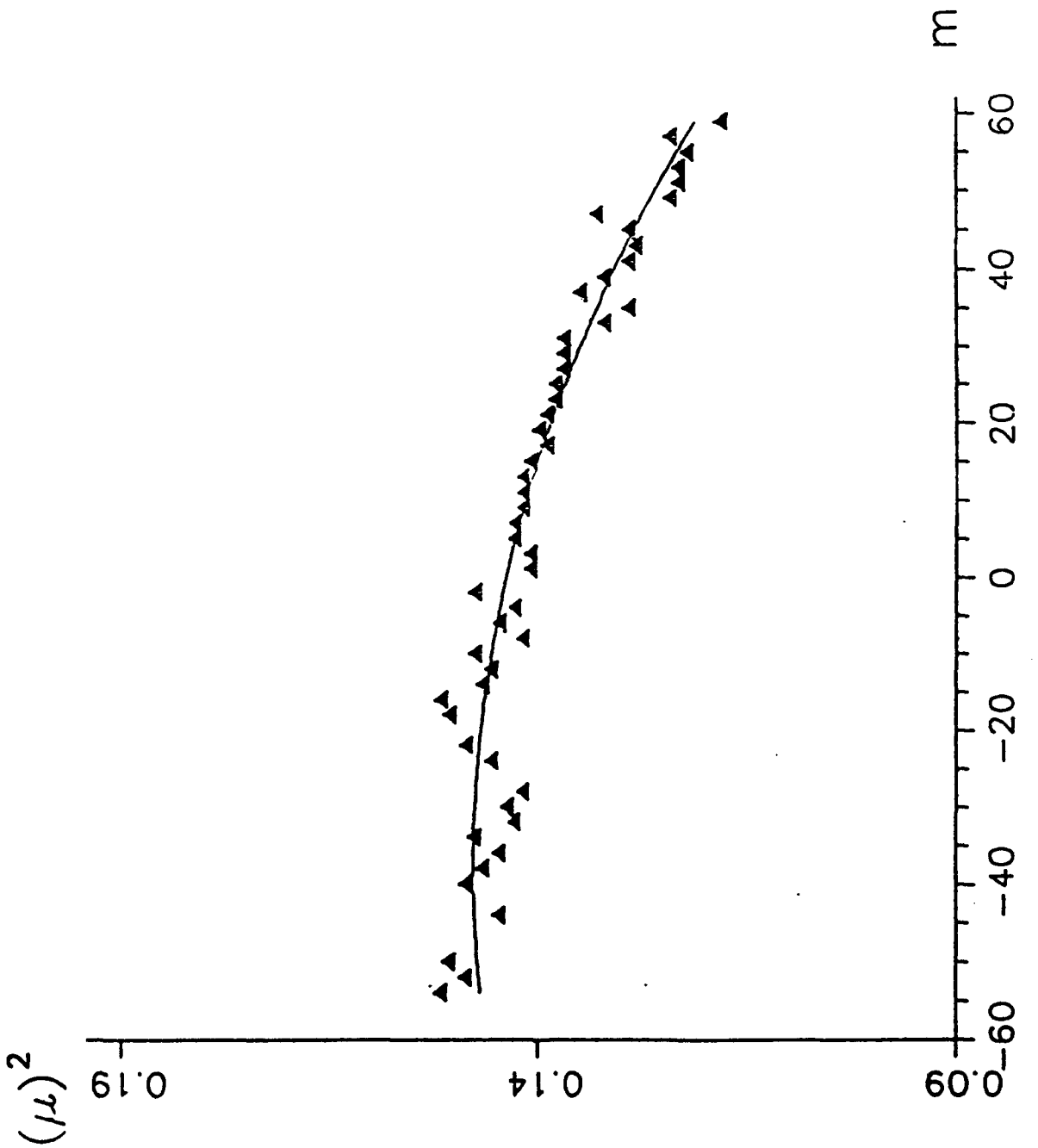

FIGURE 4

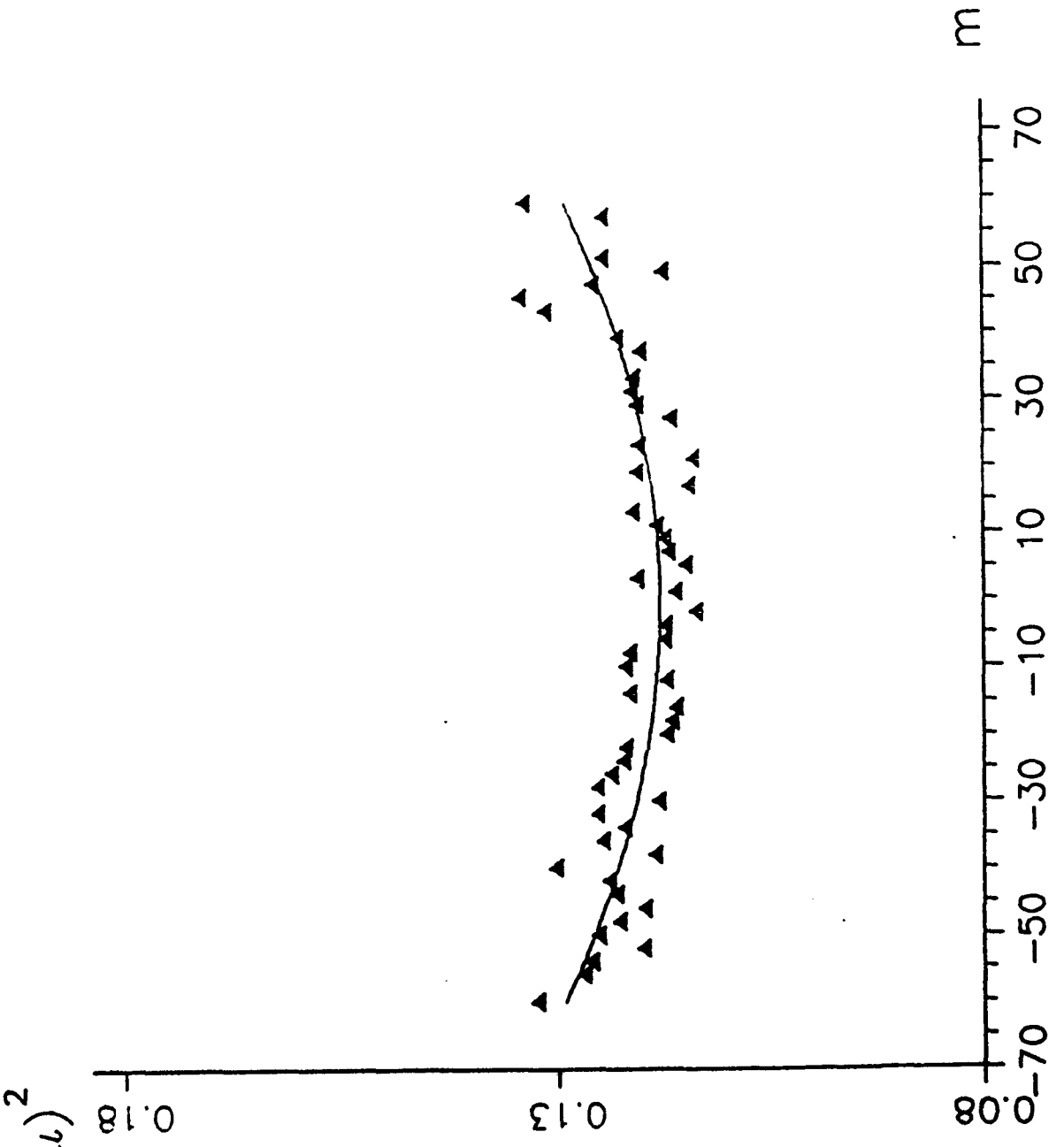

FIGURE 5

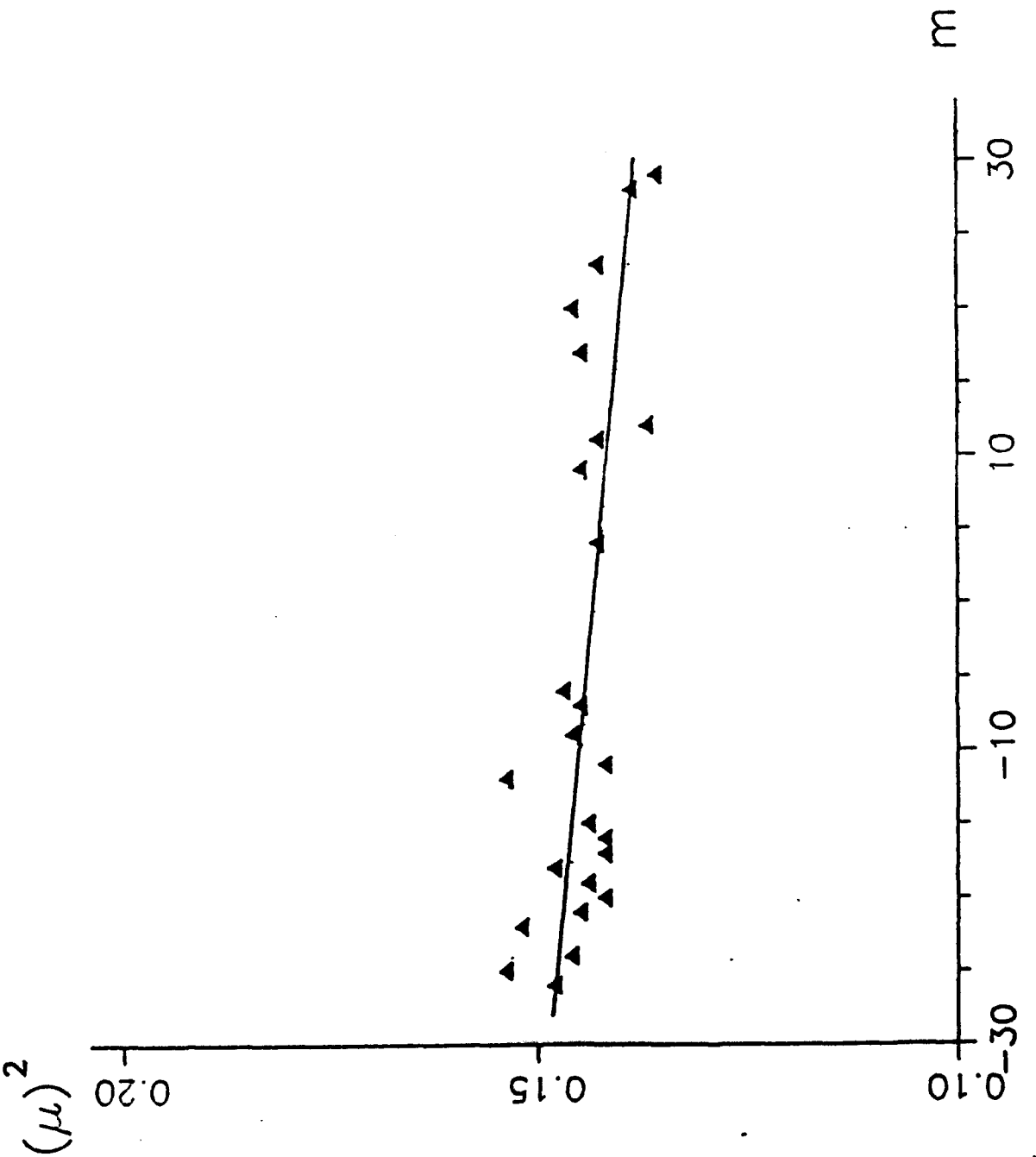

FIGURE 6

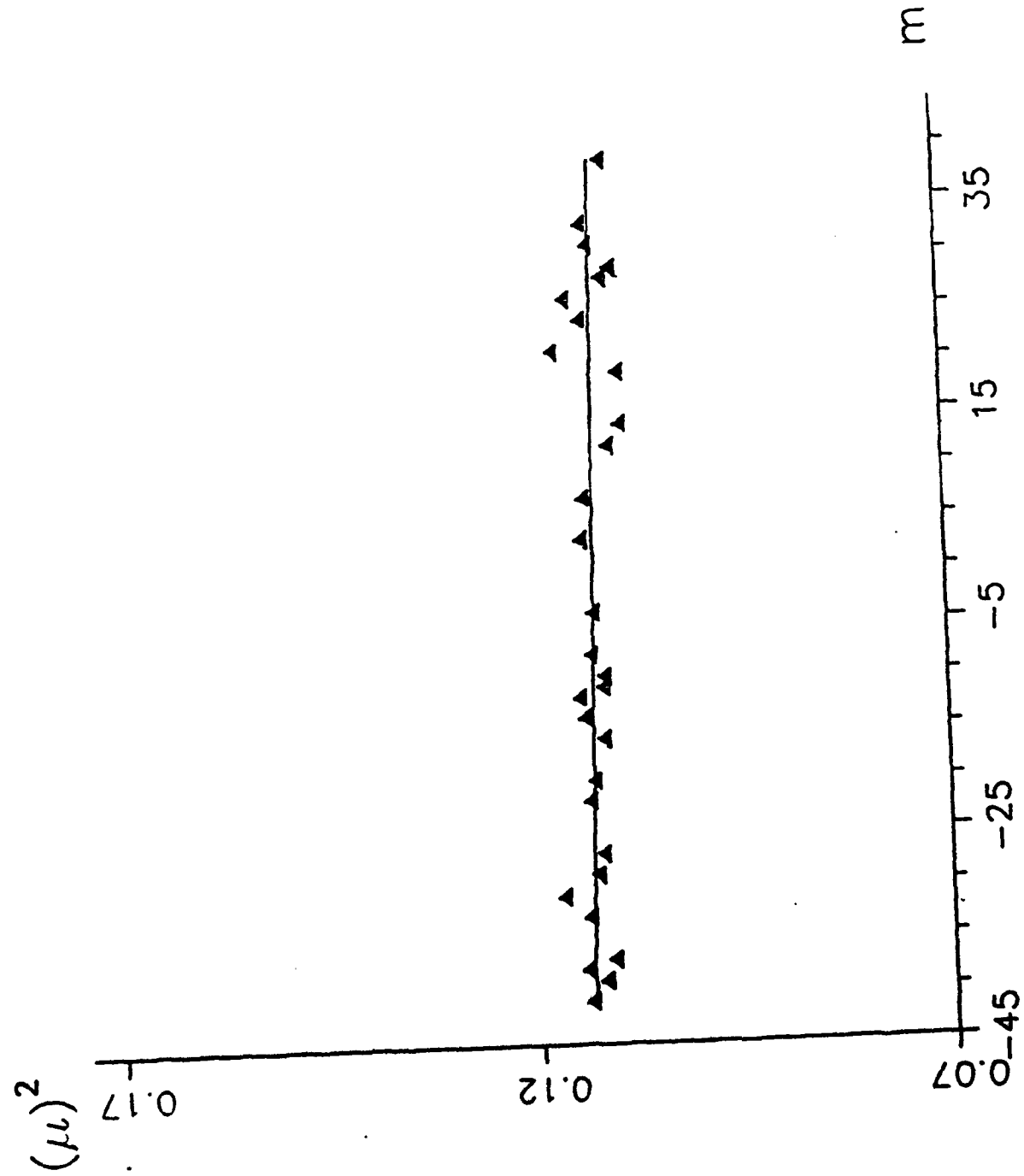

FIGURE 7

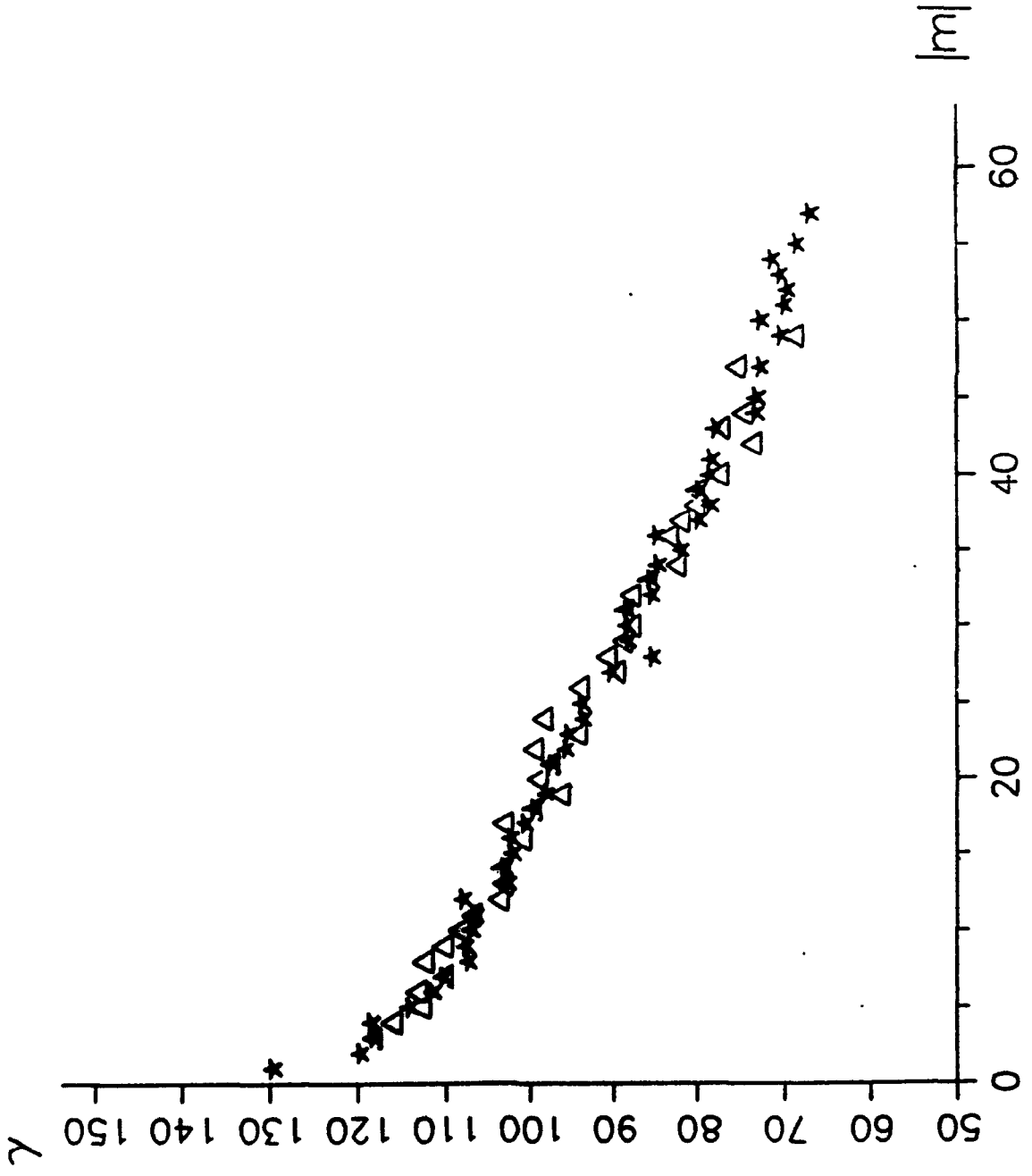

# PART II

## Intensities and Self-Broadening Coefficients of $^{13}C^{16}O_2$ Lines in the Laser Band Region

**SUMMARY**

The intensities of $^{13}C^{16}O_2$ lines have been measured in the three bands centered at 883.145, 913.425, and 1017.659 $cm^{-1}$, using Fourier transform spectra. The square of the transition dipole moment and Herman-Wallis coefficients have been determined. In addition, the self-broadening coefficients of 75 lines have been measured in the two strongest bands.

## I. INTRODUCTION

In a previous paper (1), we have studied the laser band region of the main isotopic species $^{12}C^{16}O_2$ of carbon dioxide. The study of $^{13}C^{16}O_2$, i.e. the most abundant isotopic species after $^{12}C^{16}O_2$, is also of interest for atmospheric studies and theoretical purposes. In the laser band region, $^{13}C^{16}O_2$ gives rise to two strong parallel hot bands: the 00011←10001 and 00011←10002 bands centered respectivelly at 913.425 and 1017.659 $cm^{-1}$. Another weak hot band can also be studied: it is the 01111←11101 band centered at 883.145 $cm^{-1}$. The last published experimental results concerning these bands are those of Abubakar and Shaw (see Ref. (2) and its bibliography where the references of earlier works can be found). The last published intensity calculations concerned $^{12}C^{16}O_2$: they were performed by Wattson and Rothman (3) who used a Direct Numerical Diagonalization method (hereafter denoted as DND). At the present time, the data available through the 1991 version of the HITRAN database (4) are currently used for various radiative transfer studies.

We present here the results of systematic measurements of line intensities in the three above-mentioned bands. High resolution Fourier transform spectra (unapodized FWHM = $2.7 \times 10^{-3}$ $cm^{-1}$) have been used to retrieve accurate absolute line and band intensities. The self-broadening coefficients of 75 lines pertaining to the two strongest bands could also be measured: as for the main isotopic species, they do not reveal any vibrational nor isotopic dependences.

## II. EXPERIMENTAL DETAILS

The intensity and self-broadening coefficient measurements were performed on five spectra recorded with the Fourier transform spectrometer of the Laboratoire de Physique Moléculaire et Applications, at the Université Paris-Sud. The experimental conditions are summarized in Table I.

The length of the absorption path inside the White-type cell is very well known, so that the uncertainty on this quantity (≈ 0.1%) has very small effects on the retrieved line parameters. Since hot bands have been studied in this work, it was necessary to know with a high precision the temperature of the absorbing gas. For that, the temperature was measured in three places: in the room, on the cell walls, and inside the cell. The equality of the three measured values has shown that a thermal equilibrium had been reached during the recording of each interferogram. However, as a recording takes around ten hours, small variations of the temperature occur. Then, some significant improvements were brought to the experimental setup, in order to know accurately the variation of the temperature inside the cell during the recording of the interferogram, and it was checked that these variations were very small, as it can be seen in Table I, where the uncertainties in the temperature take into account both the uncertainty due to the measurement (about 0.1 K) and the variation of the temperature. In the same way, the uncertainty of $2 \times 10^{-4}$ atm on the total pressure takes also into account the very small variations of this pressure, due to the variations of the temperature.

The $^{13}C$-enriched carbon dioxide sample used was furnished by the Sigma Chemical Company: this sample contained 99 atom % $^{13}C$ and had a minimum purity of 98%. The recorded spectra showed that this sample is actually also enriched in $^{18}O$, since the 10001←00001 band of $^{16}O^{13}C^{18}O$ centered at 1244.900 $cm^{-1}$ occurs. The concentrations of the different isotopic species have been accurately measured by mass spectroscopy, performed at the Laboratoire de Chimie Organique Structurale of the Université Pierre et Marie Curie. A R30-10 Nermag mass spectrometer was used with electron impact ionization mode (70 eV electron energy, 200 mA filament current, and 10 V repeller); the pressure of the source of $^{13}C$-enriched sample was $2 \times 10^{-7}$ torr, and the resolution was 1500. Ten experiment series, each one corresponding to an average of 50 mass spectra, were recorded in similar source conditions. Finallly, we found a concentration of $^{13}C^{16}O_2$ equal to $0.865 \pm 0.020$. This value has been confirmed by intensity measurements, performed on lines pertaining to the $^{12}C^{16}O_2$, $^{16}O^{12}C^{18}O$, and $^{16}O^{13}C^{18}O$ isotopic species.

## III. METHOD OF MEASUREMENTS

### III.1. Treatment of the channeled spectra

In the studied spectral region, fringes, caused by multiple optical reflections on the opposite sides of the beam splitter, appear on the spectra. The presence of a channel of this type is a source of difficulties in the treatment of the spectra, since it has been proved that it could hardly affect the line positions and intensities (5-7). The channel spectra were treated as in our previous work (1).

### III.2. The fitting procedure

To obtain the line parameters, a computed spectrum is adjusted to the experimental one. For that, the line shape is assumed to be a Voigt profile, calculated with the aid of the Gautschi's algorithm (8), and the apparatus function takes into account the slight apodization due to the through-put (9), as well as the asymmetry (7) depending upon the position of the studied line with respect to the channel.

The intensity of some lines cannot be measured, since in some spectral regions it was impossible to fit the channel in their vicinity, because of the presence of neighboring lines. (Note that the spectra are somewhat dense in lines, since the lines pertaining to at least four isotopic species are present.)

## IV. DATA REDUCTION AND DISCUSSION OF THE RESULTS

### IV.1. Line intensities

Using the method detailed in the previous section, we have measured one hundred of line intensities in the laser band region of $^{13}C^{16}O_2$. The five spectra (Table I) have been used, and we checked that the lines which could be measured simultaneously in different spectra does not exhibit systematic discrepancies.

Our results are reported in Tables II-IV according to the bands; the intensities have been converted to cm/mol-unit at the reference temperature of the *HITRAN* database, *i.e.*, 296 K. The uncertainty on these intensities will be discussed now. The treatment of the channel avoid large errors on the line parameters determination, but it decreases slightly the signal to noise ratio. The residuals of the fits are mainly due to the noise. On the average, the statistical relative uncertainties on the obtained intensities is 2 %. An additional uncertainty comes from the uncertainty on the temperature: several tests showed us that an error of 0.25 K on the temperature does not change the intensities by more than 1 %. The greatest source of errors is the uncertainty on the $^{13}C^{16}O_2$ concentration, *i.e.*, about 3%. On the whole, a maximum value of the uncertainty on our absolute line intensities is about 7 %.

For each band, we have derived the square of the transition dipole moment $|\mu|^2$, with respect to the running index m (m = -J" in the P branch and J"+1 in the R branch, J" being the rotational quantum number of the lower level). $|\mu|^2$ can be expressed as $|\mu|^2$

$= |\mu_0|^2 F(m)$, where $|\mu_0|^2$ is the vibrational dipole moment matrix element and F(m) the F-factor including Herman-Wallis coefficients:

$$F(m) = [1 + A_1 m + A_2 J''(J''+1)]^2. \qquad (1)$$

In addition, the relationship between the intensity of a transition between states i and f, $S_{if}$, in natural abundance, and $|\mu|^2$ is given by:

$$S_{if}(T) = (8\pi^3/3hc)\ \sigma_{if}\ [1 - \exp(-c_2\sigma_{if} / T)]\ (I_a/Q(T))\ g_n \exp(-c_2 E_i / T)\ L_{if}\ |\mu|^2\ 10^{-36}, \qquad (2)$$

where $\sigma_{if}$ is the frequency of the transition, $c_2$ is the second radiation constant (hc/k), $I_a$ is the natural isotopic abundance, Q(T) is the total internal partition sum (deduced from Ref.(10)), $g_n$ is the nuclear statistical weight of the lower level (equal to 2 for $^{13}C^{16}O_2$), $E_i$ is the energy of the lower state, and $L_{if}$ is the rotational line intensity or Hönl-London factor. The units are cgs, except for $|\mu|$ which is in Debyes. The point to be noted is that in this definition the line intensities are functions of the temperature, T, and the isotopic abundance $I_a$, while $|\mu|^2$ is independent of these quantities. The transition moment constants obtained through a fit of the line intensities are reported in Table VI. Using Eq. (2), the line intensities have been calculated and compared with their experimental values (see Tables II-IV). The agreement is good, as can also be seen on Figs. 1-3.

From the usual relationship between the band intensity and the

square of the transition dipole moment (3,11), we have calculated the intensities of the four studied bands. The obtained values are reported in Table V.

### IV.2. Self-broadening coefficients

The fitting of the line profiles can give simultaneously the line intensities and the self-broadening coefficients. This was done for the two strongest bands, but this could not be possible for the other band because of the weakness of the lines. For these weak hot lines, the self-broadening coefficients were constrained to approximate values, close to those measured in other bands.

The measured self-broadening coefficients are listed in Table VII and plotted on Fig. 4. The temperature is 293.5 ± 0.25 K, and the uncertainty on absolute values is about 5%. Figure 4 shows that for the two concerned bands, no vibrational dependence appears. One can also notice that no isotopic dependence appears, since the results concerning the two molecules $^{12}C^{16}O_2$ (1) and $^{13}C^{16}O_2$ are very close.

## V. CONCLUSION

Using Fourier transform spectra, systematic measurements of absolute line intensities have been performed in the $^{13}C^{16}O_2$ laser bands centered at 883.145, 913.425, and 1017.659 $cm^{-1}$, improving upon the previous experimental results. Also, self-broadening coefficients of lines belonging to the two strongest bands were measured. Together with our previous results (1), these new results, concerning the laser band region of the two main isotopic species of the $CO_2$ molecule, will be useful for radiative transfer studies and for theoretical purposes.

**CAPTIONS OF THE TABLES**

**TABLE I.** Experimental Conditions for the $^{13}C^{16}O_2$ spectra

**TABLE II.** Line Intensities for the 00011-10001 Band of $^{13}C^{16}O_2$

**Footnote of Table II:** Units are $10^{-24}$ cm/mol at 296 K for pure $^{13}C^{16}O_2$. $\sigma$ are the line positions in $cm^{-1}$. $S_{obs}$ are the measured intensities and $S_{calc}$ the intensities calculated using the transition moment constants listed in Table V. % is 100 x $(S_{obs} - S_{calc}) / S_{obs}$.

**TABLE III.** Line Intensities for the 00011-10002 Band of $^{13}C^{16}O_2$

**Footnote of Table III:** Units are $10^{-24}$ cm/mol at 296 K for pure $^{13}C^{16}O_2$. $\sigma$ are the line positions in $cm^{-1}$. $S_{obs}$ are the measured intensities and $S_{calc}$ the intensities calculated using the transition moment constants listed in Table V. % is 100 x $(S_{obs} - S_{calc}) / S_{obs}$.

**TABLE IV.** Line Intensities for the 01111-11101 Band of $^{13}C^{16}O_2$

**Footnote of Table IV:** Units are $10^{-24}$ cm/mol at 296 K for pure $^{13}C^{16}O_2$. $\sigma$ are the line positions in $cm^{-1}$. $S_{obs}$ are the measured intensities and $S_{calc}$ the intensities calculated using the transition moment constants listed in Table V. % is 100 x $(S_{obs} - S_{calc}) / S_{obs}$.

**TABLE V.** Transition Moment Constants $|\mu_0|^2$, $A_1$, and $A_2$ for $^{13}C^{16}O_2$

**Footnote of Table V:** $\sigma_0$ is the band center in $cm^{-1}$. The uncertainties are two standard deviations in unit of the last digit.

**TABLE VI.** Band Intensities $S_v$ of the Studied Laser Bands of $^{13}C^{16}O_2$

**Footnote of Table VI:** Units are $10^{-22}$ cm/mol at 296 K for pure $^{13}C^{16}O_2$. $\sigma_0$ is the band center in $cm^{-1}$. HITRAN'91 comes from Ref. (4)

**TABLE VII.** *Self-Broadening* Coefficients Measured for Lines of the 00011-10001 and 00011-10002 Bands of $^{13}C^{16}O_2$, in $10^{-3}$ $cm^{-1}.atm^{-1}$

**TABLE I**

---

**Radius of the iris:** 2.85 mm

**Focal length of the collimator:** 2000 mm

**Signal to Noise Ratio:** ≈ 150

**Absorbing gas:** $^{13}C$-enriched carbon dioxide, purchased from the Sigma Chemical Company, and containing 99 atom % $^{13}C$ with 98 % minimum purity. The concentration in $^{13}C^{16}O_2$ is 0.865 ± 0.02

---

| Spectrum number | Absorbing path (cm) | Total pressure ($10^{-2}$ atm) ± $2x10^{-4}$ atm | Maximal path difference (cm) | Temperature (K) |
|---|---|---|---|---|
| 1 | 417 | 5.412 | 184.19 | 293.50 ± 0.15 |
| 2 | 1217 | 5.438 | 173.06 | 293.45 ± 0.15 |
| 3 | 2817 | 5.411 | 184.19 | 293.65 ± 0.25 |
| 4 | 5217 | 5.417 | 184.19 | 293.75 ± 0.20 |
| 5 | 5217 | 5.433 | 184.19 | 293.30 ± 0.20 |

TABLE II

| Line | σ | $S_{obs}$ | $S_{calc}$ | % |
|---|---|---|---|---|
| P52 | 866.386 | 0.662 | 0.695 | -5.0 |
| P48 | 870.484 | 1.489 | 1.386 | 6.9 |
| P46 | 872.502 | 1.830 | 1.913 | -4.5 |
| P44 | 874.499 | 2.763 | 2.589 | 6.3 |
| P42 | 876.477 | 3.255 | 3.445 | -5.8 |
| P40 | 878.434 | 4.551 | 4.506 | 1.0 |
| P38 | 880.371 | 5.805 | 5.793 | 0.2 |
| P36 | 882.287 | 7.111 | 7.300 | -2.7 |
| P34 | 884.184 | 8.944 | 9.040 | -1.1 |
| P32 | 886.061 | 11.12 | 10.99 | 1.2 |
| P30 | 887.919 | 13.34 | 13.10 | 1.8 |
| P28 | 889.756 | 15.36 | 15.31 | 0.3 |
| P26 | 891.574 | 18.19 | 17.55 | 3.5 |
| P22 | 895.151 | 22.41 | 21.57 | 3.7 |
| P20 | 896.909 | 23.04 | 23.11 | -0.3 |
| P18 | 898.649 | 23.02 | 24.11 | -4.7 |
| P16 | 900.369 | 23.96 | 24.46 | -2.1 |
| P14 | 902.069 | 24.72 | 23.54 | 4.8 |
| P12 | 903.750 | 21.83 | 22.86 | -4.7 |
| P10 | 905.411 | 20.39 | 20.80 | -2.0 |
| P8 | 907.053 | 17.66 | 17.88 | -1.3 |
| P6 | 908.675 | 17.87 | 18.24 | -2.1 |
| P4 | 910.278 | 9.653 | 9.850 | -2.0 |
| R4 | 917.249 | 12.21 | 12.22 | -0.1 |
| R6 | 918.744 | 16.50 | 16.37 | 0.8 |
| R8 | 920.219 | 20.05 | 19.82 | 1.1 |
| R10 | 921.675 | 23.22 | 22.57 | 2.8 |
| R12 | 923.111 | 24.76 | 24.34 | 1.7 |
| R14 | 924.528 | 25.75 | 25.27 | 1.9 |
| R16 | 925.924 | 25.18 | 25.39 | -0.8 |
| R20 | 928.657 | 23.04 | 23.60 | -2.4 |
| R22 | 929.993 | 22.49 | 21.88 | 2.7 |
| R24 | 931.309 | 19.26 | 19.80 | -2.8 |
| R26 | 932.605 | 17.57 | 17.56 | 0.1 |
| R28 | 933.881 | 15.23 | 15.27 | -0.2 |
| R30 | 935.136 | 13.76 | 12.99 | 5.6 |
| R32 | 936.370 | 10.27 | 10.83 | -5.4 |
| R34 | 937.584 | 9.071 | 8.877 | 2.1 |
| R36 | 938.778 | 7.105 | 7.126 | -0.3 |
| R38 | 939.950 | 5.511 | 5.632 | -2.2 |

TABLE III

| Line | $\sigma$ | $S_{obs}$ | $S_{calc}$ | % |
|---|---|---|---|---|
| P58 | 960.663 | 0.171 | 0.166 | 2.7 |
| P56 | 963.002 | 0.245 | 0.245 | 0.0 |
| P54 | 965.317 | 0.350 | 0.359 | -2.7 |
| P52 | 967.607 | 0.514 | 0.517 | -0.7 |
| P50 | 969.871 | 0.747 | 0.734 | 1.7 |
| P48 | 972.110 | 1.076 | 1.024 | 4.8 |
| P46 | 974.323 | 1.383 | 1.394 | -0.8 |
| P44 | 976.510 | 1.823 | 1.881 | -3.2 |
| P42 | 978.671 | 2.607 | 2.486 | 4.6 |
| P40 | 980.805 | 3.332 | 3.240 | 2.8 |
| P38 | 982.913 | 4.140 | 4.140 | 0.0 |
| P36 | 984.993 | 4.902 | 5.216 | -6.4 |
| P32 | 989.073 | 7.732 | 7.775 | -0.6 |
| P30 | 991.072 | 9.166 | 9.243 | -0.8 |
| P28 | 993.043 | 10.73 | 10.78 | -0.4 |
| P26 | 994.986 | 11.62 | 12.29 | -5.8 |
| P24 | 996.901 | 13.59 | 13.82 | -1.7 |
| P22 | 998.788 | 15.01 | 15.12 | -0.7 |
| P20 | 1000.647 | 16.27 | 16.11 | 1.0 |
| P18 | 1002.478 | 16.48 | 16.84 | -2.2 |
| P4 | 1014.488 | 6.710 | 6.859 | -1.5 |
| R2 | 1019.961 | 5.431 | 5.309 | 2.3 |
| R4 | 1021.459 | 8.769 | 8.632 | 1.6 |
| R6 | 1022.928 | 11.66 | 11.63 | 0.3 |
| R8 | 1024.368 | 13.86 | 14.13 | -1.9 |
| R10 | 1025.778 | 15.98 | 16.05 | -0.4 |
| R12 | 1027.160 | 17.69 | 17.44 | 1.4 |
| R14 | 1028.512 | 18.16 | 18.13 | -0.1 |
| R16 | 1029.835 | 17.95 | 18.35 | -2.2 |
| R20 | 1032.395 | 17.54 | 17.24 | 1.7 |
| R22 | 1033.631 | 16.32 | 16.07 | 1.5 |
| R24 | 1034.838 | 15.07 | 14.67 | 2.6 |
| R26 | 1036.017 | 13.28 | 13.13 | 1.1 |
| R30 | 1038.289 | 10.02 | 9.825 | 1.9 |
| R32 | 1039.382 | 8.644 | 8.281 | 4.2 |
| R38 | 1042.492 | 4.554 | 4.406 | 3.2 |
| R46 | 1046.249 | 1.411 | 1.495 | -6.0 |
| R48 | 1047.120 | 1.048 | 1.093 | -4.3 |

TABLE IV

| Line | $\sigma$ | $S_{obs}$ | $S_{calc}$ | % |
|---|---|---|---|---|
| P32 | 855.527 | 0.366 | 0.378 | -3.2 |
| P29 | 858.604 | 0.505 | 0.497 | 1.6 |
| P28 | 859.273 | 0.545 | 0.537 | 1.4 |
| P27 | 860.424 | 0.560 | 0.576 | -1.8 |
| P26 | 861.115 | 0.614 | 0.615 | -0.2 |
| P24 | 862.935 | 0.695 | 0.695 | 0.0 |
| P22 | 864.734 | 0.796 | 0.763 | 4.1 |
| P21 | 865.770 | 0.799 | 0.796 | 0.3 |
| P20 | 866.513 | 0.824 | 0.822 | 0.3 |
| P19 | 867.514 | 0.815 | 0.841 | -3.2 |
| P18 | 868.270 | 0.867 | 0.860 | 0.8 |
| P17 | 869.240 | 0.872 | 0.870 | 0.3 |
| P16 | 870.007 | 0.883 | 0.870 | 1.4 |
| P14 | 871.722 | 0.876 | 0.857 | 2.2 |
| P13 | 872.634 | 0.847 | 0.841 | 0.7 |
| P12 | 873.417 | 0.825 | 0.814 | 1.4 |
| P10 | 875.090 | 0.719 | 0.730 | -1.6 |
| P9 | 875.953 | 0.672 | 0.681 | -1.3 |
| P7 | 877.584 | 0.546 | 0.560 | -2.5 |
| R4 | 886.975 | 0.389 | 0.402 | -3.3 |
| R6 | 888.470 | 0.556 | 0.543 | 2.4 |
| R9 | 890.684 | 0.676 | 0.699 | -3.4 |
| R14 | 894.240 | 0.838 | 0.808 | 3.6 |

**TABLE V**

| $\sigma_0$ | Transition | $\lvert\mu_0\rvert^2$ $10^{-3}$ Debye$^2$ | $A_1$ x $10^4$ | $A_2$ x $10^5$ |
|---|---|---|---|---|
| 883.145 | 01111-11101 | 1.702(14) | -26.4(35) | -6.9(15) |
| 913.425 | 00011-10002 | 1.841(15) | -7.8(11) | -1.09(42) |
| 1017.659 | 00011-10001 | 0.695(52) | -1.70(85) | 1.43(28) |

**TABLE VI**

| $\sigma_0$ | Transition | $S_v$ Obs |
|---|---|---|
| 883.145 | 01111-11101 | 0.00634 |
| 913.425 | 00011-10002 | 0.0907 |
| 1017.659 | 00011-10001 | 0.0633 |

TABLE VII

| Line | 00011-10001 | 00011-10002 |
|---|---|---|
| P58 | | 74.7 |
| P56 | | 70.7 |
| P52 | 70.8 | 69.6 |
| P50 | | 73.6 |
| P48 | 72.0 | 76.0 |
| P46 | 76.0 | 72.9 |
| P44 | 75.2 | 77.1 |
| P42 | 78.2 | 76.7 |
| P40 | 78.2 | 78.4 |
| P38 | | 82.0 |
| P36 | 84.0 | 77.4 |
| P34 | 84.1 | |
| P32 | 84.8 | 89.4 |
| P30 | 84.8 | 89.4 |
| P28 | 86.7 | 90.9 |
| P26 | 91.8 | 87.9 |
| P24 | | 93.1 |
| P22 | 97.0 | 96.3 |
| P20 | 93.8 | 99.9 |
| P18 | 98.1 | 98.6 |
| P16 | 100.3 | |
| P14 | 100.1 | |
| P12 | 101.3 | |
| P10 | 105.5 | |
| P8 | 104.[illegible] | |
| P6 | 109.4 | |
| P4 | 115.3 | 115.9 |
| R2 | | 127.1 |
| R4 | 110.7 | 114.1 |
| R6 | 110.9 | 108.5 |
| R8 | 106.4 | 106.9 |
| R10 | 105.5 | 105.9 |
| R12 | 101.8 | 104.9 |
| R14 | 100.7 | 100.0 |
| R16 | 97.9 | 97.8 |
| R20 | 94.1 | 97.1 |
| R22 | 91.1 | 94.4 |
| R24 | 91.8 | 94.9 |
| R26 | 89.4 | 92.9 |
| R28 | 87.8 | |
| R30 | 89.6 | 87.5 |
| R32 | 83.0 | 86.9 |
| R34 | 81.9 | |
| R36 | 79.3 | |
| R38 | 77.6 | 82.5 |
| R46 | | 66.8 |
| R48 | | 71.4 |

**CAPTIONS OF THE FIGURES**

**FIG. 1.** Variation of $|\mu|^2$ (in $10^{-2}$ Debye$^2$) vs m in the P- and R-branches of the 00011 ← 10001 band of $^{13}C^{16}O_2$. The curve represents the variation of $|\mu|^2$ calculated using the transition moment constants listed in Table V.

**FIG. 2.** Variation of $|\mu|^2$ (in $10^{-2}$ Debye$^2$) vs m in the P- and R-branches of the 00011 ← 10002 band of $^{13}C^{16}O_2$. The curve represents the variation of $|\mu|^2$ calculated using the transition moment constants listed in Table V.

**FIG. 3.** Variation of $|\mu|^2$ (in $10^{-2}$ Debye$^2$) vs m in the P- and R-branches of the 01111 ← 11101 band of $^{13}C^{16}O_2$. The curve represents the variation of $|\mu|^2$ calculated using the transition moment constants listed in Table V.

**FIG. 4.** Variation of the self-broadening coefficients $\gamma$ of $^{13}C^{16}O_2$, in $10^{-3}$ cm$^{-1}$.atm$^{-1}$, vs |m|. The measured values have been plotted as stars for the 00011 ← 10001 band, and as open triangles for the 00011 ← 10002 band.

FIGURE 1

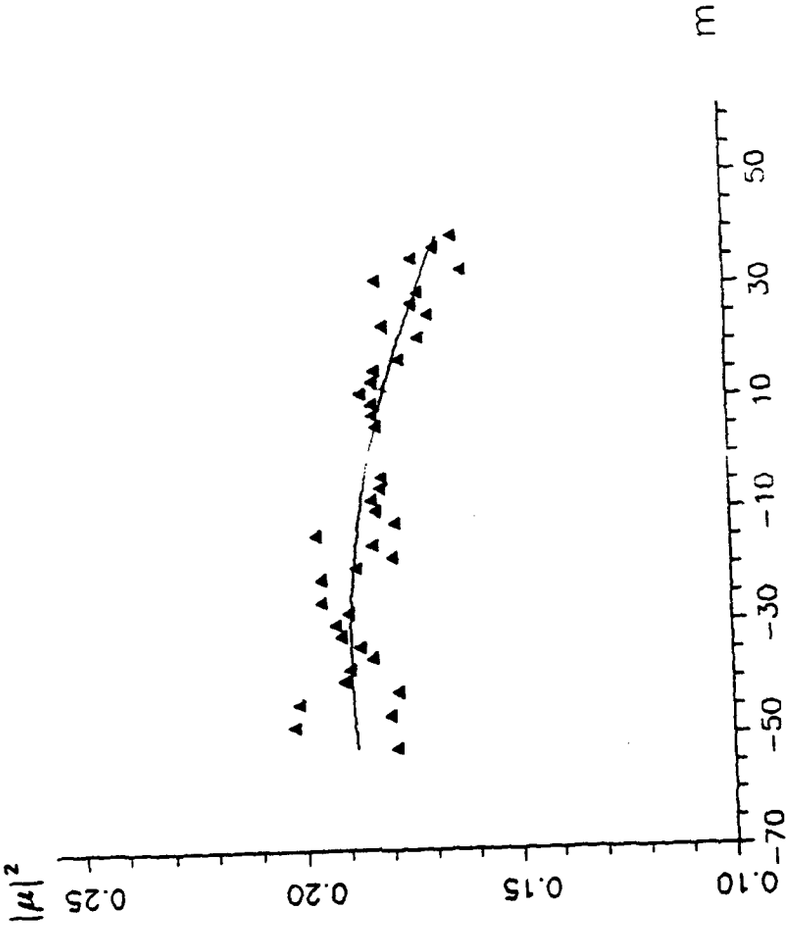

FIGURE 2

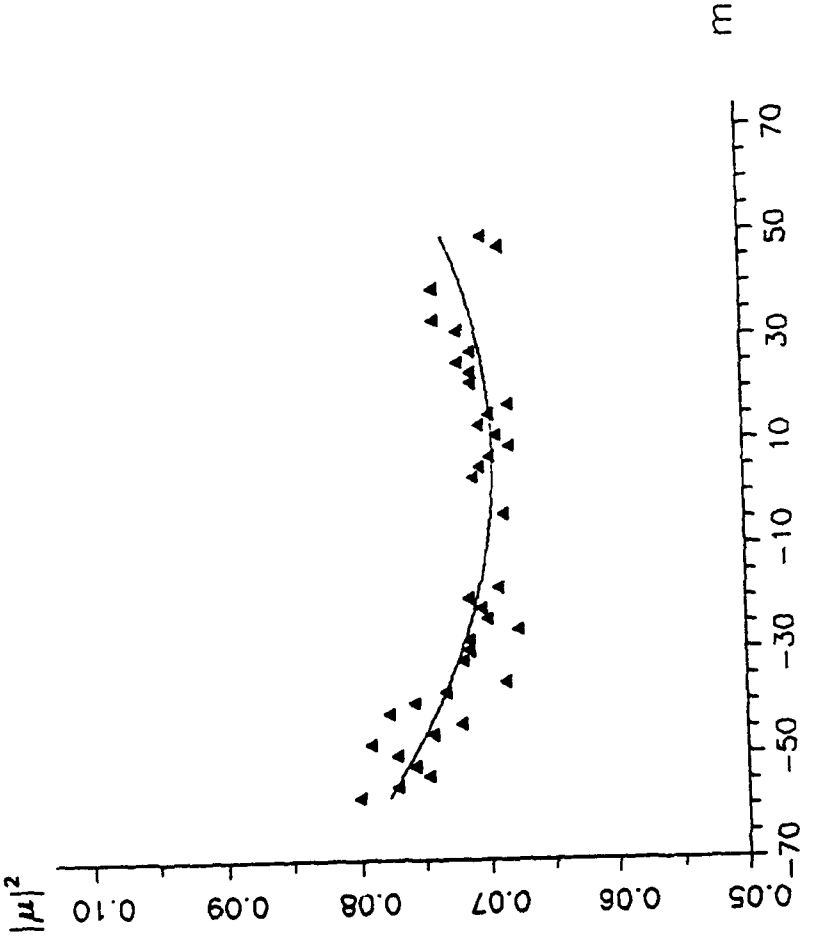

FIGURE 3

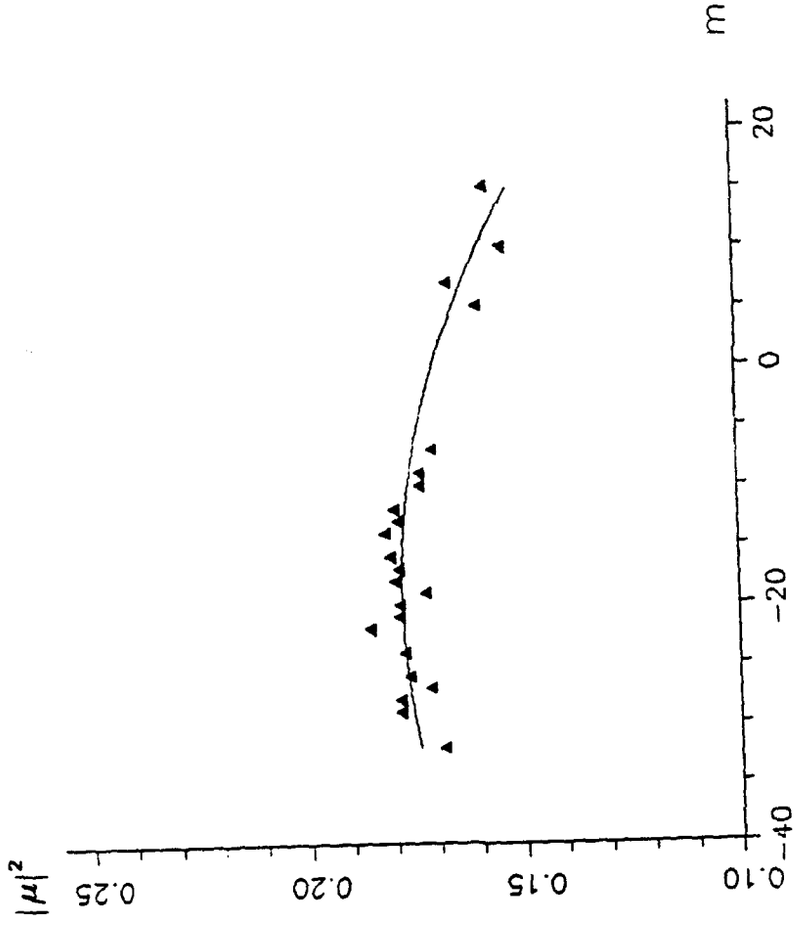

FIGURE 4

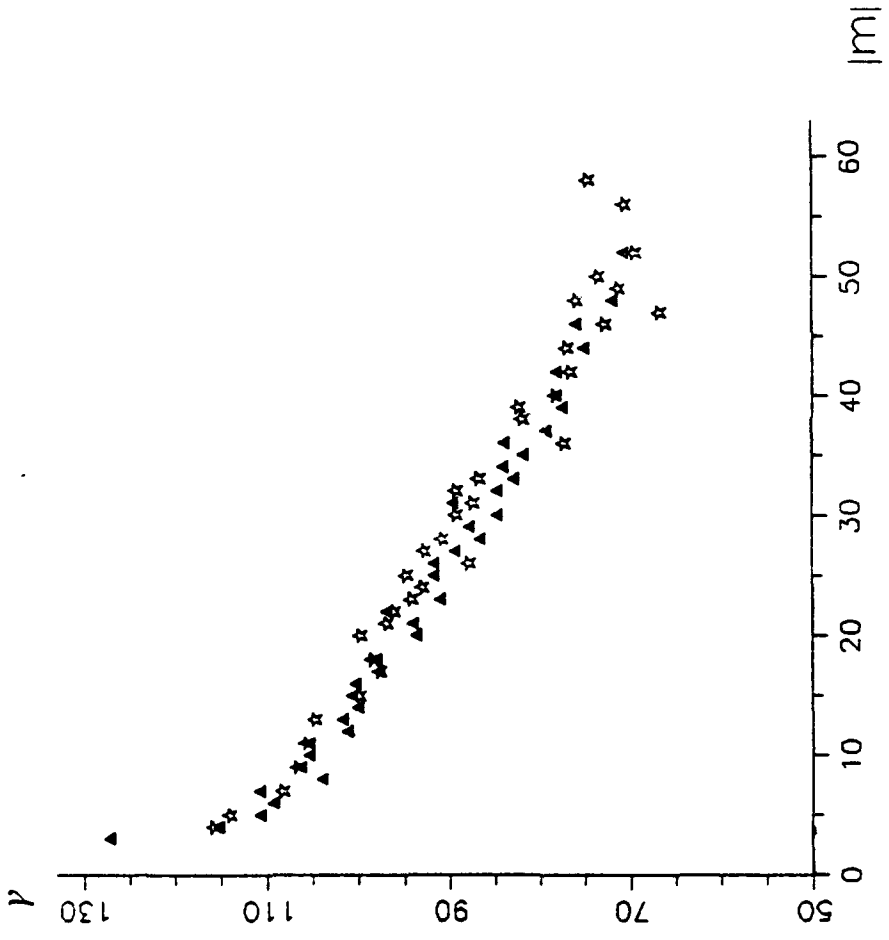

**REFERENCES**

1. V. DANA, J.-Y. MANDIN, G. GUELACHVILI, Q. KOU, M. MORILLON-CHAPEY, R.B. WATTSON, AND L.S. ROTHMAN, *J. Mol. Spectrosc.*, in press.

2. M.S. ABUBAKAR AND J.H. SHAW, *Appl. Opt.* **25**, 1196-1203 (1986).

3. R.B. WATTSON AND L.S. ROTHMAN, *J. Mol. Spectrosc.* **119**, 83-100 (1986).

4. L.S. ROTHMAN, *HITRAN Newsletter* **1**(1), 1-3 (1991).

5. G. GUELACHVILI, Thèse d'Etat, Université Paris-Sud, Orsay, 1973.

6. Q. KOU, Thèse de l'Université Pierre et Marie Curie, Paris, 1990.

7. V. DANA, J.-Y. MANDIN, A. HAMDOUNI, *Appl. Opt.*, in press.

8. W. GAUTSCHI, Communications of the ACM **12**, 635 (1969).

9. V. DANA, J.-Y. MANDIN, C. CAMY-PEYRET, J.-M. FLAUD, J.-P. CHEVILLARD, R.P. HAWKINS, AND J.-L. DELFAU, *Appl. Opt.*, in press.

10. R.R. GAMACHE, R.L. HAWKINS, AND L.S. ROTHMAN, *J. Mol. Spectrosc.* **142**, 205-219 (1990).

*11*. V. DANA, A. HAMDOUNI, R.B. WATTSON, AND L.S. ROTHMAN, *Appl. Opt.* **29**, 2474-2477 (1990).